Probing molecular dynamics with attosecond resolution using correlated wave packet pairs

Niikura, Hiromichi; Légaré, F.; Hasbani, R.; Ivanov, Misha Yu; Villeneuve, D. M.; Corkum, P. B.

Publisher's version / Version de l'éditeur:
https://doi.org/10.1038/nature01430
Nature, 421, 6925, pp. 826-829, 2003-02-20

Probing molecular dynamics with attosecond resolution using correlated wave packet pairs

Hiromichi Niikura, F. Légaré*, R. Hasbani, Misha Yu Ivanov,
D. M. Villeneuve and P. B. Corkum
National Research Council of Canada, 100 Sussex Drive, Ottawa, Ontario K1A 0R6 Canada
**Université de Sherbrooke, Sherbrooke PQ, Canada*

Spectroscopic measurements with increasingly higher time resolution are generally thought to require increasingly shorter laser pulses, as illustrated by the recent monitoring of the decay of core-excited krypton[1] using attosecond photon pulses[2,3]. However, an alternative approach to probing ultrafast dynamic processes might be provided by entanglement, which has improved the precision[4,5] of quantum optical measurements. Here we use this approach to observe motion of a D_2^+ vibrational wave packet formed during the multiphoton ionization of D_2 over several femtoseconds with a precision of about 200 attoseconds and 0.05 Angstroms, by exploiting the correlation between the electronic and nuclear wave packets formed during the ionization event. An intense infrared laser field drives the electron wave packet, and electron recollision[6-11] probes the nuclear motion. Our results show that laser pulse duration needn't limit the time resolution of a spectroscopic measurement, provided the process studied involves the formation of correlated wave packets, one of which can be controlled; spatial resolution is likewise not limited to the focal spot size or laser wavelength.

Our experiment is analogous to conventional pump-probe measurements[12], but the pump and probe occur within one optical cycle, a process that we call "sub-laser-cycle molecular dynamics" (Fig.1a). Ionization, which forms correlated wave packets around each peak of the laser field, is the pump. By removing one electron (creating an electron wave packet in the continuum), we weaken the force binding the protons and therefore launch a correlated vibrational wave packet (Fig 1b). Because of its small mass, only the electron wave packet is influenced by the laser field. In linear polarization, the electron wave packet is first moved away from the parent ion but is pulled back by the laser field. The probability of electron re-collision with the parent ion reaches a maximum at a well-defined laser phase, ~ 2/3 of an optical period after the electron's transition to the continuum (Fig. 1a). Re-collision probes the vibrational wave packet (Fig 1b). Changing the laser wavelength delays re-collision just as changing the position of a translation stage changes an optical pump-probe delay. (Neither re-collision nor the pump-probe analogy is essential: fast measurements are possible in their absence if both correlated partners are controlled, as discussed below.)

Re-collision between an electron and its parent ion has long been known as a source of high-harmonics emission[7-8,13-14] and generation of high-energy electrons[7,9]. It is also responsible for correlated multi-electron ionization in strong laser fields[7,10,13], fragmentation in small molecules[11] and attosecond pulse generation[2,3,15]. For molecules, re-collision will also imprint the spatial structure of the ion on the harmonic emission spectrum[16] or on the photoelectron spectrum[6] in analogy with conventional electron diffraction[17].

We use 40 fs laser pulses with an intensity of 1.5×10^{14} W/cm^2 tunable from 800 nm to 1850 nm. Ionization induces vertical population transfer from the D_2 ($X\ ^1\Sigma_g^+$) potential energy surface to the D_2^+ ($X\ ^2\Sigma_g^+$) surface, with less than 10^{-6} transferred to any other levels of D_2^+ (ref. 18). Since the equilibrium internuclear separation is greater for D_2^+ (1.06 Å) than for D_2 (0.74 Å), ionization initiates a vibrational wave packet motion (Fig. 1b). For all wavelengths that we use, the instantaneous ionization rate[19] is sharply peaked near the instantaneous maxima of the oscillating field. The ionization bursts last 190-300 attoseconds (800 nm - 1.85 μm). The nuclei are essentially frozen by their inertia on that time scale, ensuring that the pump stage is the same for all wavelengths

We use electron-ion re-collision to observe motion on the D_2^+ ($X\ ^2\Sigma_g^+$) surface. Although the electron returns to the parent ion several times after ionization, the first return of the electron wave packet dominates[6] and can thus be used as a probe pulse with a duration of ~ 1 fs at 800 nm (ref. 6). The time delay between the creation of the correlated wave packets and their re-collision (pump-probe delay) is controlled by varying the laser wavelength. Our delay times range from 1.7 fs to 4.2 fs (~2/3 period for λ=800 –1850 nm).

Inelastic scattering of the electron with the parent ion leads to excitation or double ionization, giving rise to the dissociative fragments of D^+. The kinetic energy of the fragments is determined by the internuclear separation at the time of electron re-collision. By using a small aperture in the time-of-flight apparatus, we observe only those fragments that originate from molecules aligned perpendicular to the laser polarization. This configuration eliminates laser-induced coupling between $X\ ^2\Sigma_g^+$ and $A\ ^2\Sigma_u^+$. Our choice of alignment ensures that the wave packet motion is simple, that it can be easily modeled and that $A\ ^2\Sigma_u^+$ is a good reference state. The existence of the well-understood reference state allows us to unequivocally interpret the kinetic energy spectrum and use it to measure the position of the vibrational wave packet.

Figure 2 shows the kinetic energy spectrum of D^+ that is due to re-collision, for all wavelengths that we have studied. Although many dissociation pathways contribute to the observed kinetic energy spectra, we can isolate the Σ_u state as particularly significant. This is because, among all inelastic scattering events from the Σ_g surface, excitation to Σ_u has the highest cross-section over the energy range examined here[20]. In addition, the Σ_u leads to fragments with the second-largest kinetic energy. Therefore this channel is easily identified in Fig. 2. We have labeled the data points that we associate with this channel with triangles. In Fig. 2 we see the motion of the wave packet reflected in the shift of this peak to lower energy with longer wavelength light.

To convert the measured kinetic energy spectrum to the vibrational wave packet on the Σ_g surface, we use the reflection principle[21]. The transformation includes the radial dependence of the collision cross-section, and a self-consistent addition of the kinetic energy of the D_2^+ Σ_g^+ wave packet, assuming that the initial average wave packet velocity is zero and initial average kinetic energy is given by the zero-point energy of D_2.

We then fit the wave packet with a Gaussian, and project back to the kinetic energy spectrum (solid curves in Fig. 2). The Gaussian fit on Σ_g determines the experimentally measured wave packet and the position of its peak. We emphasize that this is a fit to the experimental data, not a theoretical curve.

Figure 3 is a plot of the experimentally determined internuclear separation as a function of time. We represent the position of the vibrational wave packet by the peak position of the Gaussian at each laser wavelength. At each wavelength, the re-collision time is defined by the mean time for the electron wave packet's first return. This establishes the experimental points in Fig. 3. The error bars are determined by the deviation of the fit. We determine the position and the velocity of the wave packet with sub-femtosecond, sub-Angstrom resolution.

Since we are demonstrating a new technique for ultrafast measurement, it is important to compare our measurement against a standard. The solid line in Fig. 3 is the result of a simulation of the motion of a vibrational wave packet on the Σ_g surface by solving the time-dependent Schrödinger equation. The discrepancy is within the error bars.

The portion of the kinetic energy distribution that is higher than that assigned to the Σ_u state in Fig.2 corresponds to transitions to the D_2^{++} state. For 800 nm the re-collision kinetic energy is insufficient to ionize D_2^+, but at other wavelengths contribution can be seen. The peak at lower kinetic energy is not clearly identified. It contains contributions of other excited states and of the electron's multiple returns[6]. These are also seen to move to lower kinetic energies as the re-collision time is delayed.

Our current measurement accuracy is limited by noise, but noise in our data is not a fundamental limit. Using 3-D imaging detectors instead of observing through a small pinhole would increase our signal strength by about 2 orders of magnitude. A high-density jet source and a laser with higher repetition rate could further increase our signal by orders-of-magnitude.

Our method is based on the principle of creating two correlated wavepackets that could be formed on any crest of the laser field. We assert that these wavepackets are actually entangled. A field crest occurs once during each half-period throughout the 40 fs pulse. Unless the electron and vibrational wave packet are entangled, the kinetic energy spectrum for D^+ must have a 3 eV modulation (for 800 nm light, 1.5 eV per deuteron). Such modulation is well known in strong-field single-particle processes such as high harmonics generated by ionizing atomic media[8-9,13-14].

In fact, there is no 1.5 eV modulation in the kinetic energy spectrum at 800 nm in Fig. 2. We measured the spectrum with higher resolution to seek such modulation; none was observed. These experimental results are consistent with the vibrational and electron wave packets being entangled. Entanglement arises because the departing electron

contains information on the nuclear coordinate at the time of ionization and on the excited state of the D_2^+ formed in the re-collision. By observing only the deuterium ions, we integrate over all final states of other unseen, but entangled, partner particles. Such partial measurement eliminates the interference.

Regarding future applications, we note that the ultimate time resolution of correlated measurements is determined by the energy bandwidth of the electron bunch --- many tens of electron volts in the present experiment. To obtain a resolution of 200 asec will be a challenge similar to that of producing the shortest optical pulses[2].

Also, as long as both particles can be controlled, re-collision is unnecessary. For example, if two electrons are ejected into a field in a correlated fashion, the time difference between their ejection is mapped onto the final energy and angular spectra[10,15,22].

Correlated particles produced in a process with important dynamics to probe can always be measured as long as at least one of the pair can be controlled. Because of their low mass, electrons are easily controlled, while at progressively higher intensities, muons, protons, alpha particles and ions are controllable. Applying correlation to nuclear dynamics requires a means of stimulating a process such that it will occur with high probability during the duration of the intense ultrashort pulse initiating it. Nuclear processes can be stimulated in an analogous manner to inelastic scattering in our experiment --- by using a precursor molecule (such as HCl) and forcing 're-collision' between a proton and the heavy nucleus with an intense few-cycle optical pulse. To follow the subsequent dynamics, the relative trajectories of the correlated, charged nuclear fragments, as influenced by the field, can be measured.

Regarding the 'probe', we note that any method of observing the relative evolution of the correlated particles can be used for measurement. In molecular science, harmonic generation is one possible method[16] where phase matching eliminates the contribution from all but the first electron wave packet return, which occurs ~ 2/3 period following ionization. Elastic scattering is a second possible method[6], with diffraction determining the nuclear position at the time of re-collision.

Methods

Production and control of the electron wave packet

An optical parametric amplifier is used to shift the 40 fs output of a Ti:sapphire laser system to longer wavelengths. We use 800 nm, 1.2 μm, 1.53 μm and 1.85 μm pulses. Each ionizes D_2 near the field maximum and provide a progressively longer time delay between ionization and re-collision. Taking the peak of the first electron micro-bunch to be the delay time, this corresponds to delay times of 1.7, 2.7, 3.4 and 4.2 fs. Changing the wavelength has other implications. The intensity and wavelength determine the maximum re-collision energy $3.17q^2E^2/(4m\omega^2)$ of the electron [7] (q and m

are the electron mass and charge, ω and E are the laser pulse's angular frequency and electric field amplitude at the time of ionization). We use a light intensity of 1.5 x 10^{14} W/cm^2, calibrated against the ionization of xenon. While at 800 nm the peak kinetic energy of the re-colliding electron is 30 eV, the ω^{-2} scaling of the kinetic energy means that at 1.85 microns the peak re-colliding electron is ~160 eV.

Kinetic energy analysis

The kinetic energy spectrum of D^+ was measured with a time-of-flight (TOF) mass spectrometer filled with 10^{-6} Torr of D_2. The time-of-flight axis was perpendicular to the direction of propagation of the laser beam. A 1-mm diameter hole in the electrode placed 1.5 cm from the laser focus, selects only those D^+ ions resulting from dissociation of D_2^+ molecules that are aligned along the TOF axis. For the high-resolution results taken with 800 nm light (not shown), the extraction field was 133 V/cm and the acceptance angle of the TOF was 6 degrees at 8 eV. For the lower resolution results, the extraction field was 400 V/cm giving an acceptance angle of 9 degrees at 8 eV.

Selection of the re-collision channel

Deuterium ions are produced by a number of processes during strong field ionization of D_2. We distinguish fragments resulting from inelastic scattering caused by the returning electron (Fig. 2) from those produced by any other process (such as sequential double ionization [23], bond softening [24] and enhanced ionization [25-28]) using the strong sensitivity of recollision phenomena to the ellipticity of the light polarization [6-7,13]. It only takes a small ellipticity to displace the electron laterally with respect to the parent ion so recollision is impossible [7]. In strong fields, the difference between the spectrum obtained with linear and elliptically polarized light is due to recollision.

References:

[1] Drescher, M. *et al.* Time-resolved atomic inner-shell Spectroscopy. *Nature* **419,** 803-807 (2002).

[2] Hentschel, M. *et al.* Attosecond Metrology. *Nature* **414**, 509-513 (2001).

[3] Paul, P. M. *et al.* Observation of a Train of Attosecond Pulses from High Harmonic Generation. *Science* **292**, 1689-1692 (2001).

[4] D'Ariano, G. M., Presti P. L. & Paris M. G. A. Using Entanglement Improves the Precision of Quantum Measurements. *Phys. Rev. Lett.* **87**, 270404-1-270404-4 (2001).

[5] Resch, K. J., Lundeen J. S. & Steinberg A. M. Experimental Observation of nonclassical effects on single-photon detection rates. *Phys. Rev. A* **63**, 020102-1-020102-4 (2000).

[6] Niikura, H., *et al.* Sub-laser-cycle electron pulses for probing molecular dynamics. *Nature* **417**, 917-922 (2002).

[7] Corkum, P. B. Plasma perspective on strong field multiphoton ionization. *Phys. Rev. Lett*. **71**, 1994-1997 (1993).

[8] Dietrich, P., Burnett, N. H., Ivanov, M. & Corkum, P. B. High-harmonic generation and correlated two-electron multiphoton ionization with elliptically polarized light. *Phys. Rev. A* **50**, 3585-3588 (1994).

[9] Paulus, G. G., Nicklich, W., Xu, H., Lambropoulos, P. & Walther, H. Plateau in Above Threshold Ionization Spectra. *Phys Rev Lett.* **72**, 2851-2854 (1994).

[10] Weber, Th. *et al.* Correlated electron emission with multiphoton double ionization . *Nature* **405**, 658-661 (2000).

[11] Bhardwaj, V. R., Rayner, D. M., Villeneuve, D. M. & Corkum, P. B. Quantum Interference in Double Ionization and Fragmentation of C_6H_6 in Intense Laser Fields. *Phys. Rev. Lett.* **87,** 253003-1-253003-4 (2001).

[12] Zewail, A. H. Femtosecond chemistry. *Science* **242**, 1645-1653 (1988).

[13] Krause, J. L., Schafer, K. J. & Kulander, K. C. High-Order Harmonic Generation from Atoms and Ions in the High Intensity Regime. *Phys. Rev. Lett.* **68**, 3535-3538 (1992).

[14] Lewenstein, M., Balcou, Ph., Ivanov, M. Yu., L'Huillier, A. & Corkum, P. B. Theory of high-harmonic generation by low-frequency laser fields. *Phys. Rev. A* **49**, 2117-2132 (1994).

[15] Ivanov, M., Corkum, P. B., Zuo, T. & Bandrauk, A. Routes to Control of Intense-Field Atomic Polarizability. *Phys. Rev. Lett.* **74**, 2933-2936 (1995).

[16] Lein, M., Hay, N., Velotta, R., Marangos, J. P. & Knight, P. L. Role of the Intramolecular Phase in High-Harmonic Generation. *Phys. Rev. Lett.* **88**, 183903 (2002).

[17] See for example, Hargittai, I, & Hargittai, M. *Stereochemical Applications of Gas-Phase Electron Diffraction.* (VCH Publishers Inc, NY, 1998)

[18] Litvinyuk, I., Dooley, P., Villeneuve, D. M. & Corkum, P. B. unpublished results.

[19] Yudin, G. L. & Ivanov, M. Yu. Physics of correlated double ionization of atoms in intense laser fields: Quasistatic tunneling limit. *Phys Rev. A* **63**, 033404-1-033404-14 (2001); **A64** 019902 (Erratum) (2001).

[20] Peek, J. M. Inelastic scattering of electrons by the hydrogen molecule ion. *Phys.*

Rev. A **134**, 877-883 (1964).
[21] Schinke, R. *Photodissociation Dynamics 114-115* (Cambridge University Press, 1993).
[22] Itatani, J., Quere, F., Yudin, G. L., Ivanov, M. Yu., Krausz, F. and Corkum, P. B. Attosecond Streak Camera. *Phys. Rev. Lett.* **88**, 173903-1-173903-4 (2002).
[23] Lambropoulos, P. Mechanisms for Multiple Ionization of Atoms by Strong Pulsed Lasers. *Phys. Rev. Lett*. **55**, 2141-2144 (1985).
[24] Zavriyev, A., Bucksbaum, P. H., Muller, H. G. & Schumacher, D. W. Ionization and dissociation of H_2 in intense laser fields at 1.064 μm, 532 nm, and 355 nm. *Phys. Rev*. *A* **42,** R5500-R5513 (1990).
[25] Codling, K. & Frasinski, L. J. Dissociative ionization of small molecules in intense laser fields. *J. Phys. B: At. Mol. Opt. Phys.* **26**, 783-809 (1993).
[26] Seideman, T., Ivanov, M. Yu. & Corkum, P. B. Role of Electron Localization in Intense-Field Molecular Ionization. *Phys. Rev. Lett.* **75**, 2819-2822 (1995).
[27] Zuo, T. & Bandrauk, A. D. Charge-resonance-enhanced ionization of diatomic molecular ions by intense lasers. *Phys Rev*. *A* **52,** R2511-R2514 (1995).
[28] Constant, E., Stapelfeldt, H. & Corkum, P. B. Observation of Enhanced Ionization of Molecular Ions in Intense Laser Fields. *Phys. Rev. Lett.* **76,** 4140-4143 (1996).

Acknowledgements:

We acknowledge discussions with A. Stolow, A. Sokolov, A. D. Bandrauk, S. Chelkowski and J. Marangos. F. Légaré appreciates financial support from Canada's Natural Science and Engineering Research Council, the Canadian Institute for Photonics Innovation, and Le Fonds Québécois de la Recherche sur la Nature et les Technologies.

Competing interests statement: The authors declare that they have no competing financial interests.

Correspondence and requests for materials should be addressed to P.B.C.
(e-mail : Paul.Corkum@nrc.ca).

Figures Caption

Figure 1. Processes probed and exploited with the sub-laser-cycle dynamics method using correlated wave packet pairs. **(a)** Ionization forms correlated electronic and vibrational wave packets near each peak of the laser field. The vibrational wave packet **(b)** moves on the D_2^+ ($X\ ^2\Sigma_g^+$) surface while the laser field causes the electron wave packet to re-collide, represented by a thick arrow in **(a & b)**. Inelastic scattering during re-collision probes the vibrational wave packet's position. We measure the kinetic energy of the D^+ fragments **(b)**.

Figure 2. Kinetic energy distribution of D^+ at different pump-probe delay times. Shown is the experimental kinetic energy distribution of D^+ obtained using four different laser wavelengths, corresponding to different pump-probe delay times. Experimental error is estimated for each point by taking the square root of the signal counts. We identify the largest high-energy peak by the open data points with dissociation from D_2^+ ($A\ ^2\Sigma_u^+$). The curve is obtained by a fit to the data as described in the text.

Figure 3. The measured wave packet position as a function of time. To associate the laser wavelength with the time of re-collision, we use the mean time of recollision for the first electron micro-bunch at each laser wavelength. The position is determined from the peak of the fit in Fig. 2. The experimental error bars are determined by the error of the fit. The solid line is the calculated nuclear position as a function of time for a wave packet evolving on the D_2^+ ($X\ ^2\Sigma_g^+$) state. Because the time window that we measure is only about one-quarter of the full vibrational period of D_2^+ ($X\ ^2\Sigma_g^+$), the motion is almost linear.

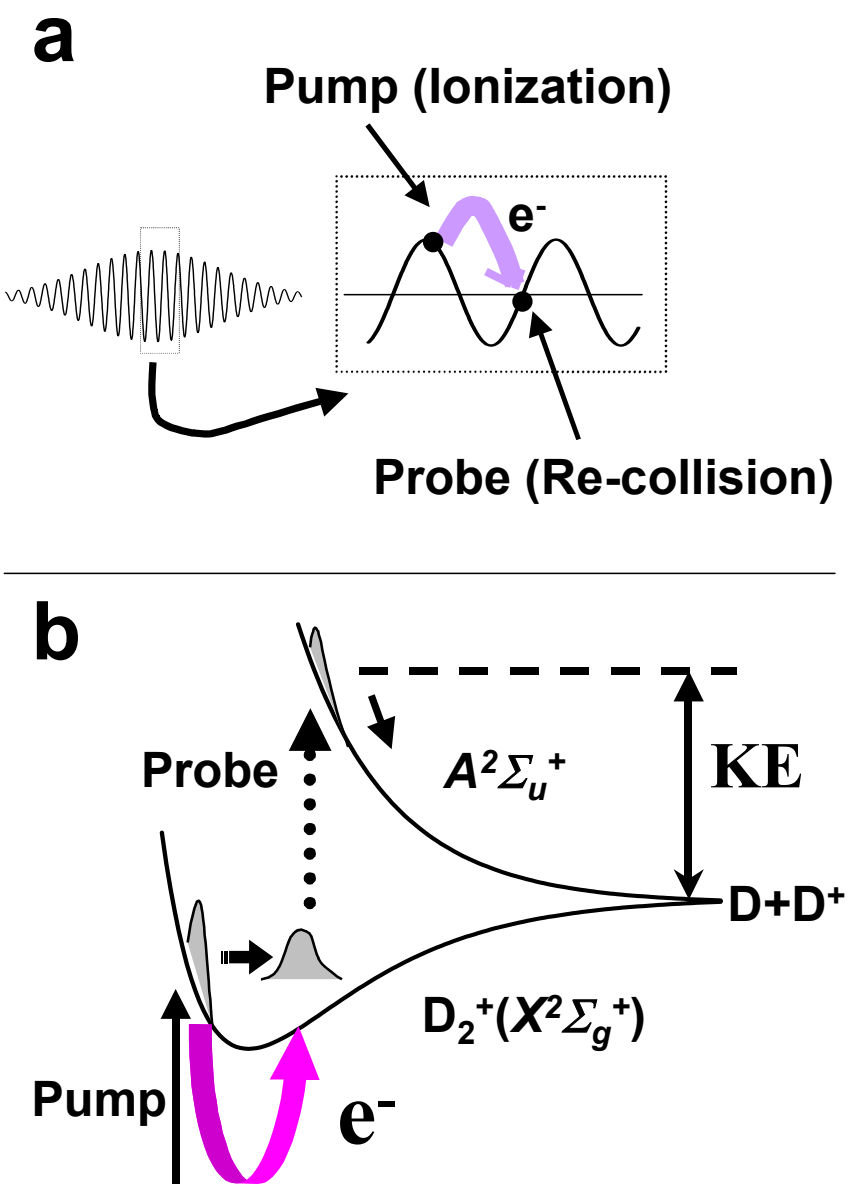

Niikura (Revision 2, 2003/01/08) Fig. 1

Niikura (Revision 2, 2003/01/08) Fig. 2

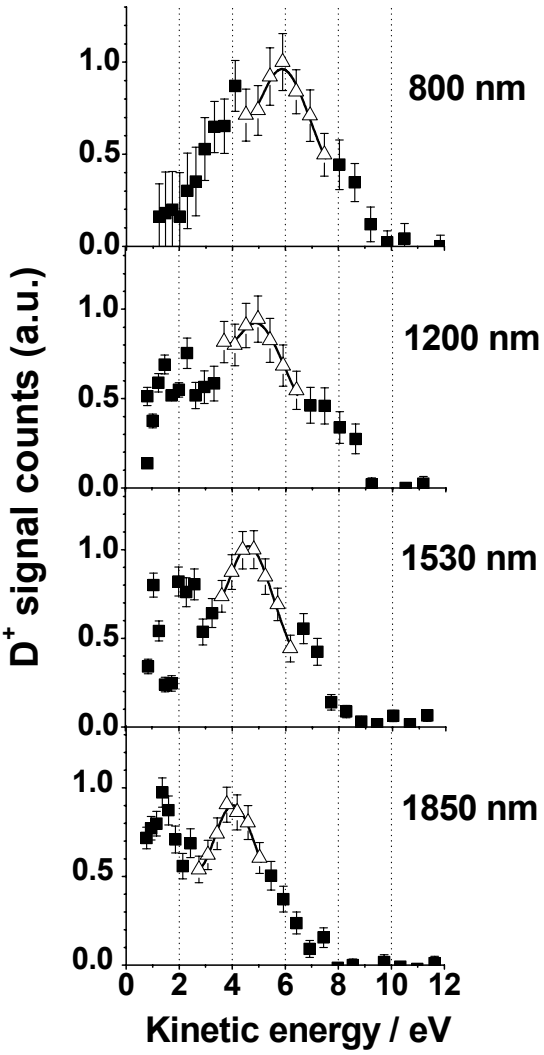

Niikura (Revision 2, 2003/01/08) Fig. 3